VI. Conclusion

The behavior of TM modes in plane metallic waveguides are quite different according to the frequency range.

For the lower frequencies, these modes are similar to those of the usual metallic waveguides. The TEM mode becomes TM_0 or a quasi-TEM mode. The other modes keep their properties. In particular, the attenuation varies like the square root of the frequency and the inverse of the dimension.

For higher frequency, the behavior of the modes are more unexpected. The TM_0 and TM_1 modes become very attenuated (the attenuation varies like ω^2). To the contrary, the other modes are far less attenuated (the attenuation varies like $\omega^{-5/2}$ and a^{-3}). This can be explained by the existence of central densities of energy, which only remain when the frequency increases. For TM_0 and TM_1 modes, this central density does not exist and these modes can't propagate any more for higher frequencies.

Our results can be used for the mixed rectangular metallic and dielectric waveguides [1], where quasi-LSE or quasi-LSM modes can be considered TE or TM modes with regard to the dielectric, and TM or TE modes with regard to the metal. The increase of the attenuation with the frequency for some low-order modes explains the poor Q coefficient for metallic cavities with respect to dielectric cavities. The same results can be obtained for circular metallic waveguides. Asymptotic expressions can be easily carried out.

References

[1] M. R. Schubert, M. S. Durschalg, and T. A. DeTemple, "Diffraction limited cw optically pumped laser," *IEEE Quantum Electron.*, vol. QE-13, pp. 455–459, 1977.

[2] J. J. Burke, "Propagating constants of resonant waves on homogeneous isotropic slab waveguide," *Appl. Opt*, vol. 9, pp. 2444–2452, 1970.

[3] D. Pasquet, "Accurate graphic resolution of the characteristic equation of a hollow dielectric slab waveguide," *Int. J. Infrared Millimeter Waves*, vol. 2, pp. 453–463, 1981.

[4] J. R. Wait and K. P. Spies, *Pure Appl. Geophys*, vol. 102, pp. 174–188, 1972.

[5] J. N. Polky and G. L. Mitchell, "Metal clad planar dielectric waveguide for integrated optics," *J. Opt. Soc. Amer.*, vol. 64, pp. 274–279, 1974.

[6] K. G. Budden and M. Eve, "Degenerate modes in the Earth-Ionosphere waveguide," *Proc. Roy. Soc. London*, vol. A342, pp. 175–190, 1975.

[7] Y. N. Lazarenko, V. F. Pavlov, and V. D. Sakhatskiey, "On some properties of surface waves in lossy media," *Radio Eng. Electron. Phys.*, vol. 21, pp. 118–120, 1976.

[8] B. Adam and F. Kneubühl, "Transversely excited 337-μm HCN waveguide laser," *Appl. Phys.*, vol. 8, pp. 282–295, 1975.

[9] E. A. J. Marcatili and R. A. Schmeltzer, "Hollow metallic and dielectric waveguides for long distance optical transmission and laser," *Bell Syst. Tech. J.*, vol. 43, pp. 1783–1809, 1964.

[10] D. Pasquet, "Waveguide discrete modes in slab and cylindrical FIR laser," *Int. J. Infrared Millimeter Waves*, vol. 2, pp. 1151–1163, 1981.

Response of Waveguides Terminated in a Tapered Metallic Wall

J. M. REBOLLAR

Abstract —**The characteristics of waveguides terminated in a tapered metallic wall are analyzed by means of the modal analysis and scattering matrix concept of discontinuities. Several applications of this kind of termination are suggested. The results can be very useful in evaluating the phase errors produced due to the use of a short-circuited waveguide with a metallic wall not placed in an exact transverse plane (z = constant).**

Manuscript received May 17, 1985; revised August 6, 1985.
The author is with the Departamento de Teoria Electromagnetica, E.T.S.I. Telecommunication, Universidad Politecnica de Madrid, Ciudad Universitaria, 28040 Madrid, Spain.
IEEE Log Number 8405932.

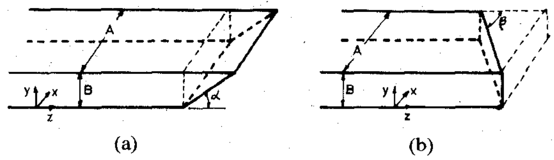

Fig. 1. Rectangular waveguides terminated in tapered metallic wall. (a) Type-"a" short circuit, slope α. (b) Type-"b" short circuit, slope β.

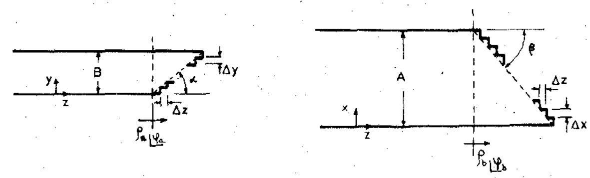

Fig. 2. Step-ladder modeling type-"a" and type-"b" short circuits, respectively.

I. Introduction

The classical way of terminating a waveguide with a metallic wall, to obtain a short circuit, is to place it in a transverse plane of the waveguide (plane z = constant). Different modes of the incident field are not generated by this termination, and the behavior of this short-circuited waveguide is well known.

However, the metallic wall can be placed, by error or by necessity, in an oblique plane.

In this paper, the effects of this kind of short circuit are studied. Two different terminations considered here are illustrated in Fig. 1(a) and (b).

II. The Model and Analysis Method

The geometry presented in Fig. 1 can be modeled by means of a step-ladder as it is shown in Fig. 2. As the steps get smaller in the limit, this model simulates properly the tapered metallic wall.

The geometries illustrated in Fig. 2 show N different waveguide sections of Δz length, terminated in a classical short circuit with metallic wall in a transverse plane.

These configurations can be exactly analyzed by means of a new technique combining the model analysis and scattering matrix concept of transverse discontinuities [1]–[3]. The electromagnetic field in each waveguide section is assumed to be the sum of their eigenmodes. Then the scattering matrix S of each discontinuity is obtained [3]. Finally, all discontinuities are joined in order to obtain the exact response of the complete structure by a method similar to that proposed by Patzelt and Arndt [3]. This method permits the combination of as many discontinuities as desired. The number of modes used to describe the electromagnetic field in each waveguide section can be as large as permitted by the computer. However, convergence is quickly obtained and 20 modes are enough to solve the problem.

The exciting field from the left is considered to consist of the fundamental TE_{10} mode of the rectangular waveguide. With this incident field, and considering the step discontinuities of the "a" and "b" cases, the next modes are considered.

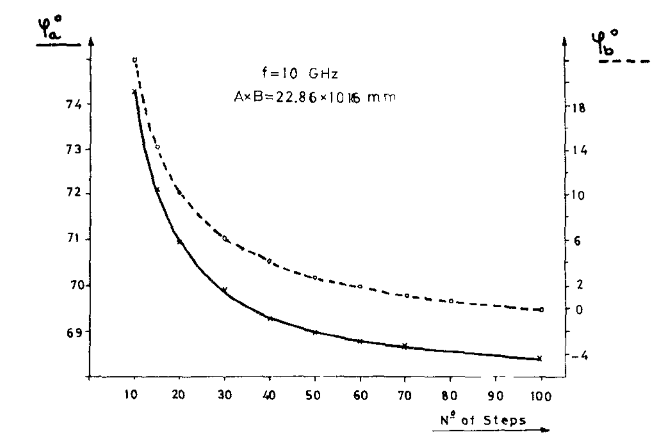

Fig. 3 Reflection coefficient phase of short circuits. type "a" (φ_a ——, $\alpha = 45°$), type "b" (φ_b----, $\beta = 45°$) versus number of steps.

TABLE I
COMPARISON BETWEEN NUMERICAL RESULTS OBTAINED BY CAMPBELL AND JONES [4] AND THIS METHOD

K_g B	φ_a,[4]	φ_a(this method)
0.2π	143°	144°
0.35π	112°	112°
0.5π	71°	72°
0.65π	13°	15.6°

K_g: guide wavenumber

A. Termination Tapered in Height of Waveguide, Type-"a" Short Circuit (Fig. 1.(a))

Only discontinuities between rectangular waveguides with different heights exist; therefore, only the $TE^x_{1,n}$ family of modes is considered. Other authors consider both $TE^z_{1,n}$ and $TM^z_{1,n}$ to solve these kinds of discontinuities. The results obtained with both family of modes are the same.

B. Termination Tapered in Width, Type-"b" Short Circuit (Fig. 1(b))

In this case, discontinuities between rectangular waveguides with different widths are considered; only the $TE^z_{n,o}$ family of modes are excited.

III. Numerical Results

First, the influence of the number of steps N on the phase of the reflection coefficient is studied. In Fig. 3, the phase of the reflection coefficient (φ_a and φ_b) is shown versus the number of steps. In the cases presented, the slopes are $\alpha = 45°$ and $\beta = 45°$. The dimensions of the input waveguide are $A \times B = 22.86 \times 10.16$ mm, and the frequency is 10 GHz.

As can be seen in this figure, when the number of steps is increased, the phase of reflection coefficient shows a good asymptotic behavior of short circuits "a" and "b."

The case of a type-"a" short circuit with $\alpha = 45°$ has been dealt with as a special case of a truncated right-angle E-plane corner by Campbell and Jones [4]. In Table I, results from [4] and the ones obtained by this method are presented. A very good agreement can be observed between both methods.

The modulus of the reflection coefficient obtained in all cases of short-circuit type "a" is unity at the frequency band 7–14 GHz. This is due to the fact that the all modes generated ($TE^x_{1,n}$, $n \geq 1$) are evanescent modes in this frequency band. However, in short-circuit type "b," the modulus of the reflection coefficient is less than 1 when the $TE^z_{2,0}$ is propagating. For example, $\rho_{TE_{10}} = 0.911\angle -177.8°$ at 14 GHz for $\beta = 45°$.

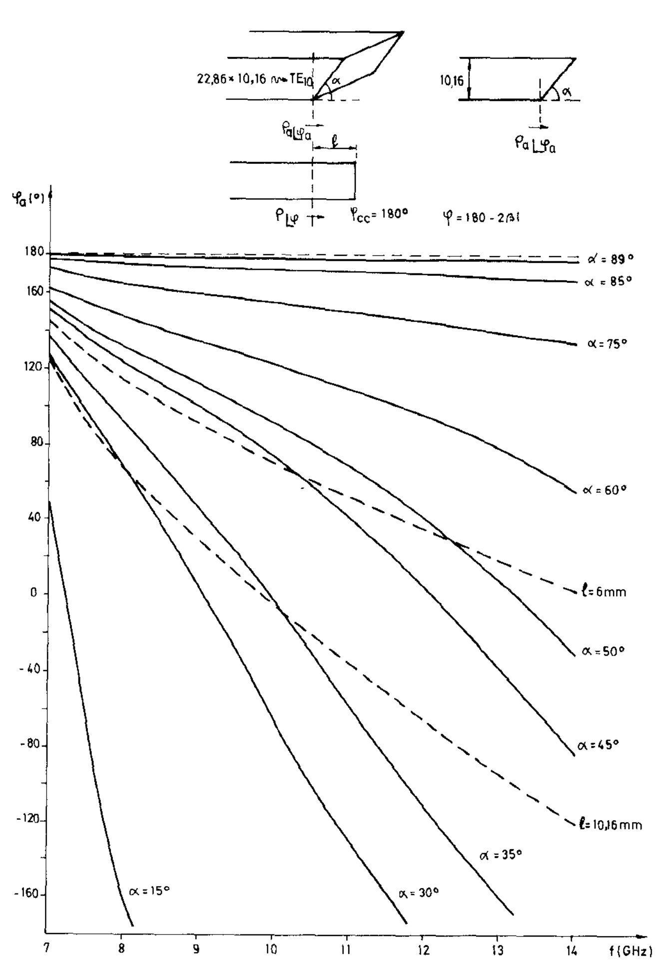

Fig. 4. Reflection coefficient phase of type-"a" short-circuit (φ_a) for different slopes (——), and for classical short circuits $\alpha = 90°$ at distance l from the metallic wall (----).

The phase response (φ_a and φ_b) at the frequency band 7–14 GHz for different slopes (α, β) of the short circuit are shown in Figs. 4 and 5 (dimensions of the input waveguide are $A \times B = 22.86 \times 10.16$ mm).

The typical response of a short circuit ($\alpha = 90°$) at distances l($l = 6$ mm and $l = 10.16$ mm) from the terminal metallic wall can be seen in Fig. 4. From this plot, it can be seen that the phase lines of $\alpha = 90°$, $l = 6$ mm, and $\alpha = 50°$ have different slopes. Using this property, a circuit composed of a waveguide section plus a short circuit with slope α can give a linear phase response over the entire frequency band of the waveguide. An example is shown in Fig. 6. It can be seen that the phase line of the combination of the type-"a" short circuit ($\alpha = 50°$) and a waveguide section of length 6 mm is nearly a linear function of frequency. Also presented in Fig. 6 is the phase line of a waveguide section of length 11 mm terminated in a classical short circuit ($\alpha = 90°$). A nonlinear dependence with the frequency can be observed due to dispersion of the propagation constant.

The response of the type-"b" short circuit is quite different from the type "a." This different behavior can be explained taking into account that the fundamental mode TE_{10} is never under its cuttoff frequency in the type-"a" short circuit. How-

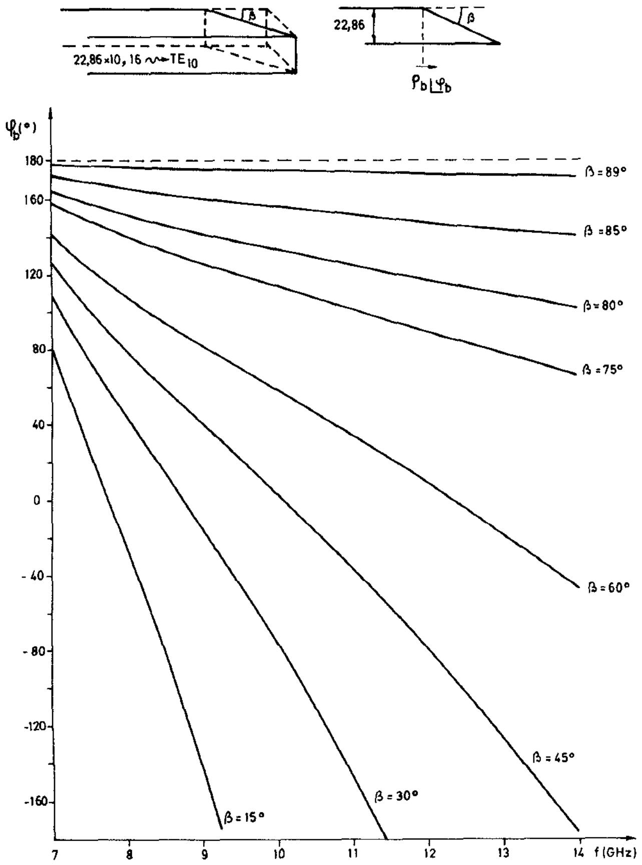

Fig. 5. Reflection coefficient phase (φ_b) of type-"b" short circuits for different slopes.

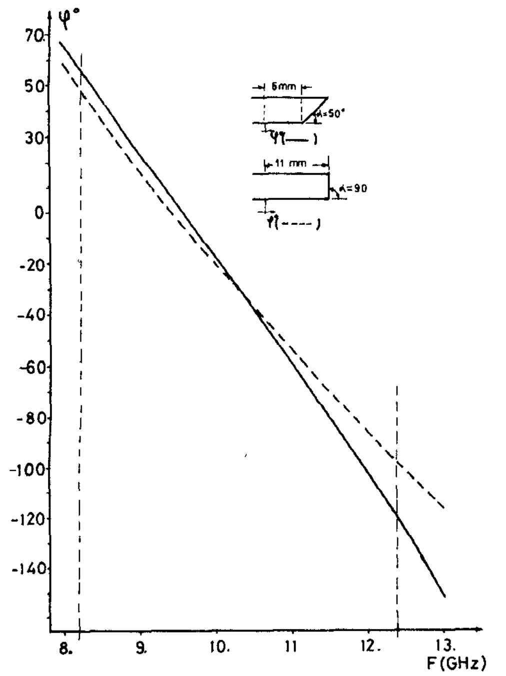

Fig. 6. Reflection coefficient phase of the combination of type-"a" short circuit ($\alpha = 50°$) and rectangular waveguide section (22.86×10.16 mm) of 6-mm length (———), and classical short circuit $\alpha = 90°$ at distance $l = 11$ mm from the metallic wall (----).

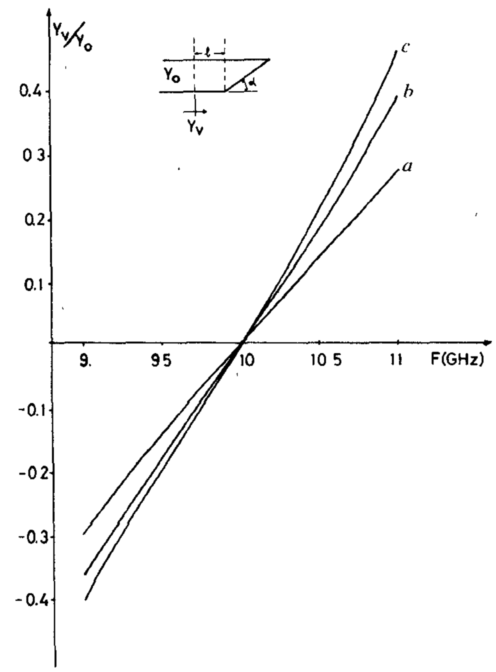

Fig. 7. Normalized input admittance of waveguide sections (length l) plus short-circuit type "a" (slope α). a: $\alpha = 90°$, $l = 9.939$ mm. b: $\alpha = 45°$, $l = 3.810$mm. c: $\alpha = 40°$, $l = 2.200$ mm.

ever, in type "b," the dominant mode is an evanescent field in the final part of the tapered waveguide.

The plots shown in Figs. 4 and 5 give an idea of the phase error due to an incorrect construction of a typical short circuit ($\alpha = 90°$). It can be seen that an error of one degree in the type-"b" short circuit ($\beta = 89°$) causes the phase to become 175.1° at $f = 10$ GHz instead of the expected 180°.

These waveguides terminated in a tapered metallic wall can be used for filter designs. If a $\lambda_g/4$ stub terminated in a short circuit ($\alpha = 90°$) is considered, the input admittance at the designed frequency is zero. The normalized input admittance of this stub is presented in Fig. 7 (case a). The normalized input admittance of two different combinations of the waveguide section plus the slope shortcircuit are also shown. Note that the slope of the admittance $dY/d\omega$ is greater in these two last cases. This behavior is useful in obtaining filters with higher Q.

IV. Conclusions

Waveguides terminated in a tapered metallic wall have been analyzed. The proposed model and the employed method to solve the problem have been shown to be very efficient.

The obtained results show the possibility of employing these terminations to achieve a linear phase response, avoiding the dispersion of the propagation constant. Another application may be the design of filters with higher Q.

The results presented are useful to evaluate phase measurement errors due to incorrect construction of short circuits.

Acknowledgment

The author is indebted to Dr. J. E. Page for his helpful suggestions and he wishes to thank the reviewers of this paper.

References

[1] A. Wexler, "Solution of waveguide discontinuities by modal analysis," *IEEE Trans. Microwave Theory Tech.*, vol. MTT-15, pp. 508–517, Sept. 1967

[2] P. H. Masterman and P. J. B. Clarricoats, "Computer field-matching solution of waveguide transverse discontinuities," *Proc Inst Elec. Eng.*, vol. 118, no. 1, pp. 51–63, Jan 1971.
[3] H. Patzelt and F. Arndt, "Double-plane steps in rectangular waveguide and their application for transformers, irises and filters," *IEEE Trans. Microwave Theory Tech.*, vol. MTT-30, pp. 771–776, May 1982
[4] J. J. Campbell and W J. Jones, "Symmetrically truncated right-angle corners in parallel-plate and rectangular waveguides" *IEEE Trans. Microwave Theory Tech* , vol MTT-16, pp 517–529, Aug. 1968.

A Method for the Calculation of Exact Capacitances of Circular Rod Arrays

SHIMON CASPI

Abstract —**An exact solution of the capacitance matrix of circular rods located inside a grounded rectangle is presented. The capacitances were determined by solving the integral equation for the charge densities on the conductors using the Green function. The results are compared to E. G. Cristal's [1] data. Examples of the computing capacitance matrix for some unsymmetrical configurations are given.**

I. Introduction

Using circular rods in building microwave components (filters, couplers) is very popular because of its manufacturing advantage as compared to rectangular bars. The capacitances of rods as a function of geometrical dimensions were calculated by E. G. Cristal [1]. He solved the problem for the important and particular case where the rods are located on the axis of symmetry between ground planes, using the following assumptions: 1) Coupling beyond nearest neighbors is negligible, 2) A moderate change in the size or spacing of a given rod has only a second-order effect on the charge distribution on the far side of adjacent rods.

The purpose of the present paper is to solve the above problem generally, i.e., for any configuration of the rods between ground planes and without usage of Cristal's assumptions.

II. Method

The method used to determine the capacitance matrix is by solving an integral equation for the charge densities on the conductors, and using the Green's function as a Kernel [2], [3]. The form of the Green's function used is the one suggested by Chestnut [3], which is convenient for numerical work and takes into account the effect of finite side walls.

The difficulty in solving the integral equation is the logarithmic singularity point in the Green's function. It is necessary to solve a limit problem N times for every rod (N—number of points in the numerical net).

Manuscript received March 1, 1985; revised August 13, 1985
The author is with Department 3405, ELTA Electronics Industries Ltd., P O B 330, Ashdod 77102, Israel.
IEEE Log Number 8405933

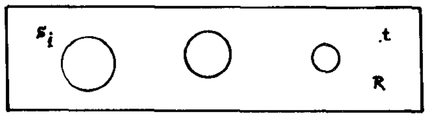

Fig. 1. A system of n conductors

In the present paper, we solve the limit problem analytically, enabling us to obtain an integral equation that is as simple as an ordinary integral equation.

A. The Integral Equation

Following Chestnut [3], we define the problem: Let $\phi j(t)$ be the function satisfying the following boundary value problem:

$$\nabla^2\phi j(t) = 0 \text{ in } R,$$
$$\phi j(t) = 1 \text{ on conductor } S_j,$$
$$\phi j(t) = 0 \text{ on conductor } S_i,\ i \neq j,$$
$$\phi j(t) = 0 \text{ on the boundary of the rectangle,}$$

where t is a point (x, y) in region R, R is the region interior to ground planes, and S_i is the surface of conductor i (see Fig. 1). Using the concept of the Green's function, we get

$$V_j = \sum_{i=1}^{N} \int_{\partial S_i} G(t, t') Q_j(t')\, dS$$

where V_j is $\phi j(t)$ on the surface S_j, G is the Green's function, and Q_j is $\partial\phi j/\partial n$, the charge density on the conductors.

This is a set of n equations for n unknown functions. Solving it will give the capacitance matrix by $C_{ij} = \epsilon \int_{\partial S_i} Q_j(t)\, dS$.

B. The Numerical Solution

By the Gaussian quadrature formula, the integral equation is reduced to a matrix equation [3]

$$B\overline{Q} = \overline{V}$$

$$b_{ij} = \begin{cases} \omega_j G(t_i, t_j), & i \neq j \\ \omega_i D_i + \dfrac{1}{2\pi} \displaystyle\sum_{\substack{k=1 \\ k \neq i}}^{Ni} \omega_k \cdot \ln|t_i - t_k| - \dfrac{Ei}{2\pi}, & i = j \end{cases}$$

$$t_i = x_i + \pi, \quad \omega_i = \frac{2\pi}{(1 - X_i)^2} P_{N'}(X_i)^2$$

where X_i is zeros of the Legendre polynomial and P_N is the Legendre polynomial

$$E_i = \int_0^{2\pi} \ln|t_i - t|\, dt = 2\pi \ln(r) \quad \text{(on a circular rod)}$$

$$D_i = \lim_{t \to t_i} \left(G(t_i, t) + \frac{1}{2\pi} \ln|t_i - t| \right)$$

and the capacitance will be

$$C = \epsilon \sum_{k=1}^{N_i} \omega_k \cdot Q(t_k).$$